phys. stat. sol. (b) **222**, 63 (2000)

Subject classification: 61.72.Lk; 62.20.Fe; S5.11; S7.12

Low Temperature, High Stress Plastic Deformation of Semiconductors: The Silicon Case

J. RABIER[1]) and J.L. DEMENET

Laboratoire de Métallurgie Physique, UMR 6630, CNRS, Université de Poitiers, SP2MI, BP 30179, F-86962 Futuroscope-Chasseneuil Cedex, France

(Received April 3, 2000)

Dedicated to Professor Dr. Wolfgang Schröter on the occasion of his 65th anniversary

Low temperature deformation experiments of silicon under confining pressure are analyzed with reference to a possible transition at high applied stress τ_t between dissociated glide configuration and perfect shuffle as extrapolated from the calculations of Duesbery and Joos (Phil. Mag. Lett. **74**, 253 (1996)) as well as the low temperature deformation experiments on compound semiconductors (CSC). It is shown that experiments performed at a higher value of the expected transition stress have not put forward the evidence of such a transition. The influence of a preexisting population of glide dislocations on such a transition in the deformation mechanisms is also discussed.

1. Introduction

Low temperature high stress plastic deformation tests have been performed in semiconductors with the aim of investigating deformation regimes such as decorrelated partial movements, twinning as well the effect of electronic doping. Indeed at low temperatures, point defect diffusion is limited and the importance of doping is expected to be greater, the lower the deformation temperature is. In order to achieve such low temperature deformation regimes, two techniques can be used which superimpose an hydrostatic component on the shear stress which enables a shift in the brittle to ductile transition down to lower temperatures: microindentation and deformation under a confining pressure. The first of these techniques is very easy to handle but suffers from two main drawbacks: the stress tensor is not known and the plastic region is localized in a very small part of the specimen, which makes the TEM observations of the deformation substructure difficult. The second one enables a control of both the deviatoric and hydrostatic stresses and allows for the observation of the deformation microstructure in the whole sample. In this context experiments have been performed some time ago in Si and GaAs as a function of doping and compression axis orientation [2–5].

Since then calculations in Si have put forward quite convincingly that a glide shuffle transition can occur at high stresses. Indeed calculations of the Peierls stress [6] deduced from γ surface computations [7] confirm that the Peierls stress is larger in the glide set than in the shuffle set. The Peierls stress has been found to be 0.35μ (μ shear modulus [8]) for 30° partials in the glide set and 0.1μ for screw dislocations in the

[1]) Corresponding author; e-mail: Jacques.Rabier@lmp.univ-poitiers.fr

shuffle set. These results seem irrelevant when compared to experimental results which show that dislocations are dissociated, i.e. belong to the glide set. However, by calculating the elastic energy required for double kink nucleation, including the Peierls barriers dislocations need to overcome, Duesbery and Joos [1] have shown that the movement of a dissociated dislocation in the glide set has a lower activation energy than the movement of a perfect screw dislocation in the shuffle set in the usually investigated range of stress. Nevertheless, the calculations show that perfect dislocation movement in the shuffle set can have a lower activation energy at high stresses.

Recently it has proved possible to increase quite extensively the temperature range investigated in the III–V compounds and to deform GaAs, InP and InSb under a confining pressure down to the liquid nitrogen temperature at 1.2 GPa [9]. This increase in the plastic range investigated has led to the observation of a hump in the $\sigma(T)$ curves. Furthermore, a transition clearly appears in the plot of $\ln(\tau)$ versus $1/T$. The microstructures which consist mainly of perfect screw dislocations below the transition temperature have been interpreted as the occurrence of a glide–shuffle transition. However, no calculations have been done yet in III–V CSC to confirm the occurrence of this transition that was predicted for silicon.

As far as silicon is concerned it appears very difficult to increase substantially the temperature range of plasticity using the standard techniques of deformation under a confining pressure. The lowest temperature achieved with Si was 275 °C even after predeformation at higher temperatures under a pressure of 1.5 GPa which is the highest pressure that can be achieved with a standard Griggs apparatus [10]. However, extrapolating the data of Duesbery and Joos shows that the transition stress between a deformation mechanism controlled by dissociated glide dislocations and a deformation mechanism controlled by perfect shuffle dislocations should occur at stresses close to 0.01μ, i.e. about 680 MPa. Such stresses have been already reached in experiments that have been recalled before [2, 3].

In this context, the aim of the present paper is to re-analyse the data on low temperature deformation of Si in the light of the Peierls stress calculations in Si and the results obtained on CSC, stressing on the differences between Si and CSC materials.

2. Experimental Results

This section recalls the results previously obtained on silicon and CSC about mechanical data and deformation microstructure observations. Only the more important features in relation with the present paper are reported.

2.1 Stress–strain curves

Figure 1 shows the stress–strain curves obtained at low temperatures on a virgin crystal of Si [2, 3] and GaAs [4, 5]. The Si curve exhibits the usual yield point which is characteristic of Si deformation at higher temperature. This bears witness to a low dislocation density, a multiplication stage and an overshoot in the dislocation density. On the other hand, the GaAs curves show a parabolic hardening stage as soon as the yield stress is reached which is different from deformation at higher temperatures on the same material, i.e. with the same as-grown dislocation density. This has been interpreted [11] by the fact that, at low temperatures, screw dislocation segments become far

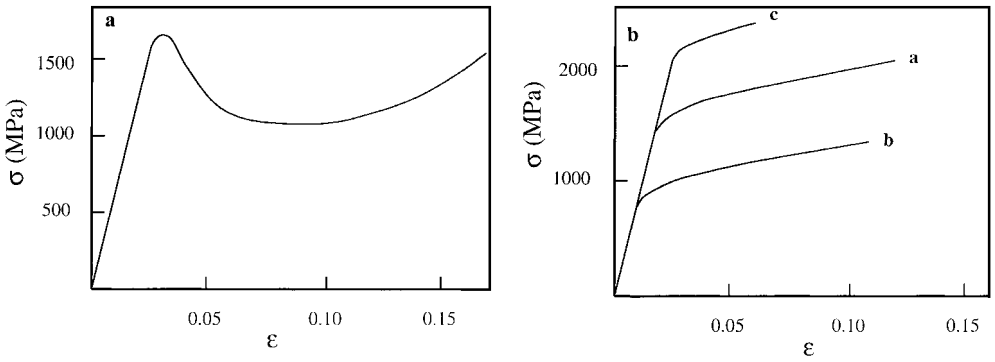

Fig. 1. a) Stress–strain curve of Si deformed at $T = 425\,^{\circ}\mathrm{C}$ and $\dot{\varepsilon} = 2 \times 10^{-6}\,\mathrm{s}^{-1}$, under a confining pressure of 700 MPa. b) Stress–strain curves of (a) intrinsic, (b) n-type and (c) p-type GaAs deformed at room temperature and $\dot{\varepsilon} = 2 \times 10^{-5}\,\mathrm{s}^{-1}$, under a confining pressure of 1.4 GPa

slower compared to the other dislocation segments. As a consequence the nucleation stage is less efficient than at higher temperatures and yields to a hardening effect.

GaAs, InP and InSb have been shown to plastically deform down to liquid nitrogen temperature without any pre-deformation under a confining pressure of 1.2 GPa [9]. This is different from Si for which the lowest test temperature achieved at 1.5 GPa was 275 °C provided that the sample had been pre-deformed at a higher temperature. In this case the stress–strain curve does not show a yield point anymore but a parabolic hardening stage.

2.2 TEM observations

Microstructures obtained on deformed Si samples with ⟨123⟩ and ⟨100⟩ compression axes are very different. Indeed the resolved applied stress on the easiest glide plane is such as to lead to a diminution of the dissociation width for ⟨123⟩ and to an enlargement for the ⟨100⟩ axis.

Figure 2a shows the microstructure obtained after deformation of a ⟨123⟩ sample up to the upper yield stress (τ = 800 MPa) at 450 °C under a hydrostatic pressure of

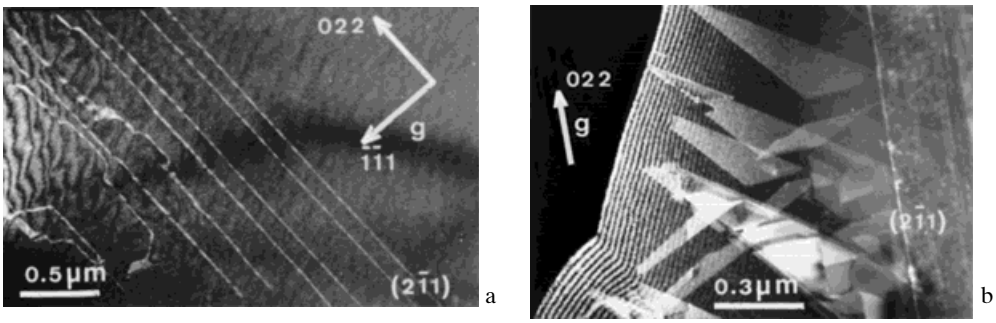

Fig. 2. Microstructure of Si after deformation along a) ⟨123⟩ up to the upper yield stress (τ = 800 MPa); b) ⟨100⟩ up to the lower yield stress (500 MPa). Deformation conditions: $T = 450\,^{\circ}\mathrm{C}$, confining pressure 1.5 GPa, $\dot{\varepsilon} = 2 \times 10^{-6}\,\mathrm{s}^{-1}$

1.5 GPa and a strain rate of 2×10^{-6} s^{-1}. In the primary glide plane the microstructure consists of dissociated dislocations. There is a tendency for the screw segments to be longer than the other ones. However, this microstructure is not very different from what is found at higher temperatures under standard deformation conditions. Moreover, although the stress tensor favours the narrowing of the stacking fault, no perfect dislocations are obtained. So there is no evidence for the existence of perfect shuffle dislocations even though the stress applied is larger than the expected stress for the incidence of the glide–shuffle transition.

As far as the microstructure of the ⟨100⟩ sample is concerned, it consists of extended stacking faults in accordance with a deformation mechanism controlled by the movement of decorrelated partials, Fig. 2b.

2.3 Yield stress as a function of temperature

Two types of analysis can be made to understand the variation of yield stress with temperature,

$$\dot{\varepsilon} = \dot{\varepsilon}_0 \exp -(\Delta G/kT), \tag{1}$$

$$\dot{\varepsilon} = A\sigma^n \exp -(Q/kT) \; . \tag{2}$$

The first one, which is well suited for high stress mechanisms, was used by Castaing et al. [2]. The stress dependence of the activation free energy was determined by stress relaxation tests and was found to be logarithmic. Then the variation of the yield stress can be written as

$$\ln(\tau) = \ln(\tau_0) + bT \tag{3}$$

where the strain rate dependence is introduced in b (Fig. 3). The flow stress at 0 K, τ_0, lies between 100 and 200 GPa, in the order of magnitude of the shear modulus, and $\Delta G/kT = c$, with $c = 36$. This large value of c is unexpected; a reasonable value for c should lie between 20 and 30 [12].

Although Eq. (2) is only strictly valid at high temperatures, the use of such a relation for a range of high stress–low temperature can be useful for comparing high stress and low stress ranges. Indeed by plotting $\ln(\tau)$ versus $1/T$, a change in slope is evidenced for high stresses in CSC. Such a plot has been made for Si, Fig. 4 [13]. There is a bend in the plot for high stresses. However, by comparing with the change in the plots of III–V CSC, Fig. 5, it can be seen that the tempera-

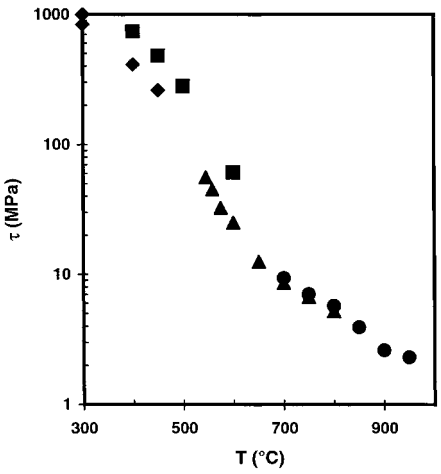

Fig. 3. Variation of the lower yield stress of Si with temperature. ◆ and ■ Castaing et al. [2], ● and ▲ Omri et al. (see [2] for references)

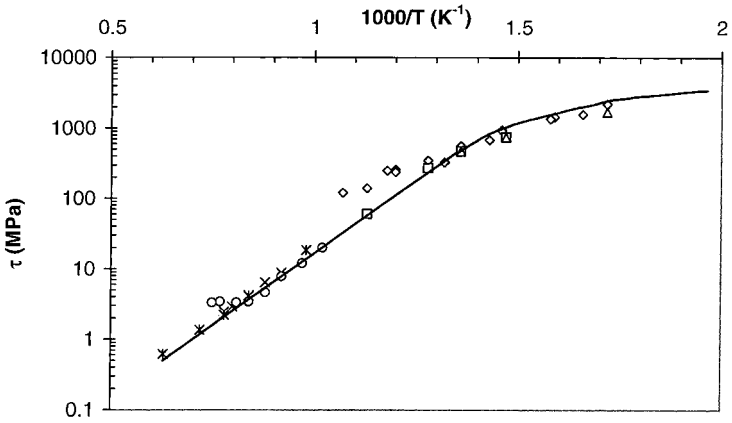

Fig. 4. Silicon: lower yield stress as a function of temperature, from [13]. ⁎ Siethoff, ○ Omri et al., × Yonenaga and Sumino, □ and △ Castaing et al. See [13] for references. The data from Demenet [14] (◇) have been added

ture range investigated in Si is far too small to make a valid comparison. This remark is also consistent with the fact that from TEM observations there is no apparent change in the deformation mechanism in ⟨123⟩ samples. Another interesting point is that although the deformation mechanism is different for ⟨123⟩ and ⟨100⟩ oriented samples, as revealed by TEM observations, the yield stresses for the two orientations lie on the same master curve.

The yield stress obtained in Si as a function of temperature down to 275 °C can be compared with the microhardness data obtained down to room temperature by using a

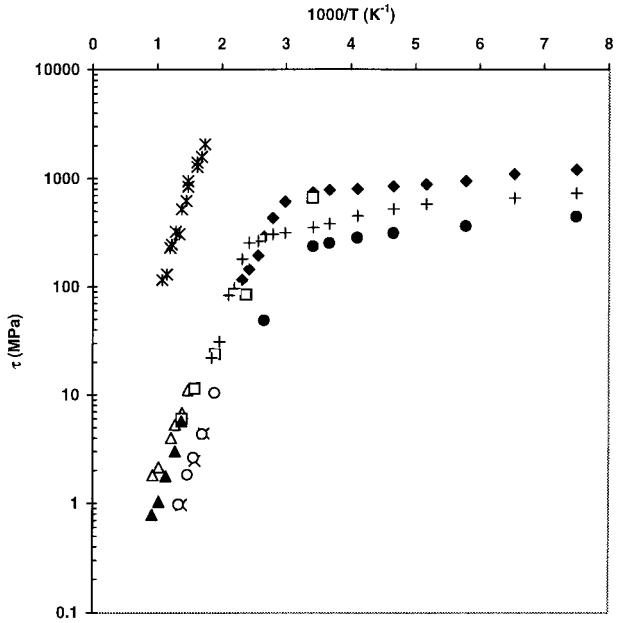

Fig. 5. Logarithm of τ as a function of $1/T$ for three III–V compounds, from Suzuki et al. [9]. GaAs: □, ◆ and △; InP: +, ▲ and ×; InSb: ○ and ●. For references, see [9]. The data from Demenet [14] (⁎) on Si have been added

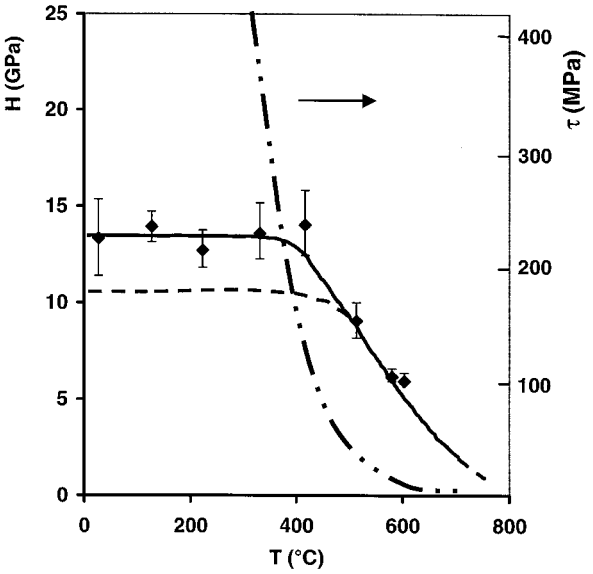

Fig. 6. Silicon: hardness as a function of temperature, from [15]. The variation of the yield stress as a function of temperature from [2] is also schematically drawn

$\tau = f(T)$ plot, Fig. 6 [15]. In contrast to the yield stress, microhardness values level off below 400 °C. This has been attributed to the phase transition encountered under the indentor which appears at 12 GPa [16, 17]. Indeed with this mechanical test it is impossible to decorrelate the hydrostatic component of the stress tensor from the uniaxial one. This phase transition can be avoided during compression under a hydrostatic pressure provided the pressure is kept to a lower value than that required for the phase transition. However there is no report until now on the extension of the plasticity range of Si by using higher hydrostatic pressures.

3. Discussion

3.1 On the bend in the plot of ln (τ) versus 1/T

Extending the range of plasticity of CSC leads to a transition in the plastic properties at a low temperature [9]. This transition appears clearly in a plot of ln (τ) versus $1/T$ below a temperature T_c. Usually, this plot is linear with a slope proportional to the activation energy for dislocation glide in the material. Similar plots were found by the group of Cleveland in 4H SiC and 6H SiC [18, 19].

The interpretation is based upon the fact that below T_c only the more mobile dislocations, assumed to have a lower activation energy, are nucleated. This is the case if a glide–shuffle transition is supposed to occur (CSC) or when the movements of partial dislocations become decorrelated (SiC).

However, the basic mechanisms are quite different. In the glide–shuffle transition mechanism, the dislocation core is expected to be modified and it is the slowest segment of the glide loop which controls the deformation. In the case of a transition from correlated to decorrelated partial dislocation movement, it is the fastest segment (or several fast segments) which controls the deformation. Indeed, expanding a glide loop creates new dislocation segments with different orientations and characteristics. In this

view the source shuts off when the expansion yields to the appearance of segments possessing a higher activation energy. This problem can be avoided if surfaces are taken into account thus preventing slower partial segments to participate in the loop expansion. In SiC it has been assumed that the leading partial with the lower activation energy is nucleated and that trailing partial only starts to nucleate at or above T_c when thermal activation becomes sufficiently large [19].

Since a bend is seen on the plot of $\ln(\tau)$ versus $f(1/T)$, irrespective of whether the deformation occurs by correlated partials or decorrelated partials, it is of interest to compare partial loop expansion in Si with that in CSC. In what follows it is assumed that it is the α/β character which is relevant to this problem in CSC whereas in Si only the differences in mobility between 30° and 90° partial has to be taken into account. α partials are assumed to be the fastest in compounds and the 90° partials in Si in relation with dislocation velocity measurements [20].

A dislocation loop in semiconductors is composed of dissociated segments lying along the ⟨110⟩ directions in the (111) glide plane. Figure 7a shows a glide loop in Si consisting of 90° and 30° partials. To this geometrical character is added in CSC the α/β character, Fig. 7b. Considering the geometrical configuration of a leading partial loop in Si and CSC, its expansion requires the movement of the different sets of partials in which appear the slowest ones, i.e. the 30° segment in Si and the β segment in CSC. From this it is clear that the expansion of a whole partial loop requires the same activation energy as the expansion of a dissociated loop. Now if we consider nucleation of partial dislocation loops from the surface, one has to consider the velocity of adjacent segments. In Si a fast segment is always found in between two slow segments whereas in CSC three fast segments can be found adjacent, Fig. 7. A comparison of nucleation geometry for Si and CSC can then be considered starting from this point. These consist, respectively, of a half loop composed of 30° partials bounding a 90° segment in Si (Fig. 8) and a half loop composed of three α partials for CSC (Fig. 9). It is easy to figure out the expansion of such surface loops. For Si the displacement of the fastest 90° partial yields to its disappearance so that the two slow 30° partials remain. Further movement needs a larger activation energy. In CSC the expansion of the surface source can be achieved only with the fastest partials.

From these mechanisms, based on the assumption of surface sources, it is clear that plasticity by partial dislocations can be achieved with a lower energy than perfect dislocations in CSC. In Si the activation energy is the same for the two

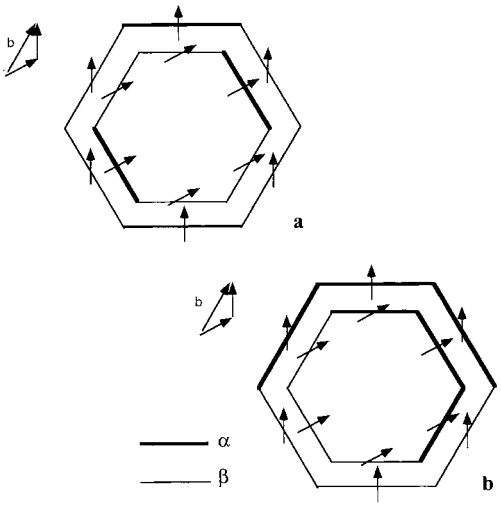

Fig. 7. Glide loop in Si and CSC; fastest dislocation segments are in bold. a) Si: 90° segments are the fastest, b) CSC: α segments are the fastest

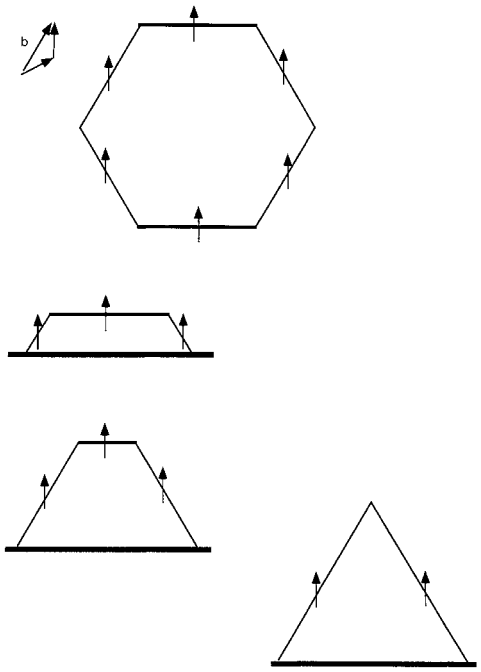

Fig. 8. Surface source in Si constituted of 30°/90°/30° segments. Successive stages of expansion of the loop yield to the locking of the source by slow 30° segments

regimes of deformation. These conclusions are in agreement with the fact that in Si, high stress deformation regimes controlled by dissociated dislocation movement ($\langle 123 \rangle$ compression axis) or by decorrelated partials movement ($\langle 100 \rangle$ compression axis) have the same activation energy.

The bend in the plot of $\ln(\tau)$ versus $1/T$ in Si cannot be related either to a change in mechanism from correlated partials to decorrelated partials or to a glide–shuffle transition as shown by TEM experiments. Rather the actual curvature can be explained by the shape of the $\Delta G = f(\tau)$ curve without any change in mechanism in the plotted range. Nevertheless it is of interest to calculate what could be the effect of the change in dislocation core (glide to shuffle) on the yield stress behaviour as a function of temperature. Indeed free energy calculations for 30° glide partial and perfect screw shuffle show that a change in mechanism has to occur at about $10^{-2}\mu$ (Fig. 10). From these free energy values, a plot of the yield stress as a function of $1/T$ can be extracted using Eq. (1) since it leads to $\Delta G(\tau) = ckT$. Using this relation and a reasonable value of c ($c = 24$) and the value deduced from Castaing et al. [2], the yield stress has been plotted as a function of $1/T$ for the two core hypotheses, Fig. 11. This leads to transition temperatures of about 600 and 315 °C in these two cases ($c = 24$ and 36, respectively). This hypothesis cannot be forwarded since no change in microstructure relevant to such a core transition has been found in the whole bend domain.

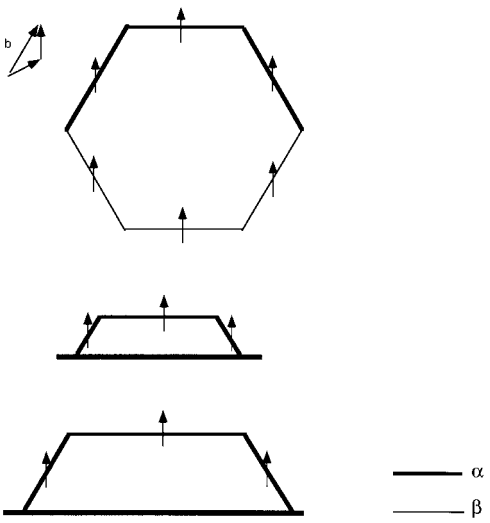

Fig. 9. Surface source in CSC constituted of α/α/α segments. Successive stages of expansion of the loop are controlled by the displacement of rapid α segments

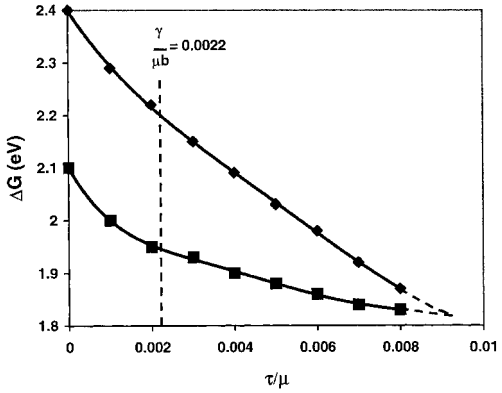

Fig. 10. Free energy for kink pair nucleation and migration for a 30° glide partial (■) and a screw shuffle (◆) dislocation as calculated by Duesbery and Joos [1]. τ_t, the transition stress between the two mechanisms, is about 0.01μ. The minimum stress required for glide partial decorrelation is also indicated

3.2 From glide to shuffle: the influence of a pre-deformation

Although yield stresses larger than the calculated transition stress have been obtained without pre-deformation, no evidence of a deformation controlled by perfect shuffle dislocations was obtained. By pre-deforming, larger yield stresses can be obtained without obtaining any evidence of perfect dislocations. From these observations, it seems that the transition stress is far larger than that calculated or that it is difficult to obtain a shuffle population from a pre-existing glide one. This pre-existing population could shift the transition stress to larger values.

Starting from pre-existing glide dislocations, two situations can occur:

– The stress required for partial decorrelation [13],

$$\tau_d = \frac{2\gamma}{b}\,\frac{1}{\dfrac{1-R^*}{1+R^*}-f}\,, \tag{4}$$

with γ the stacking fault energy and b the perfect Burgers vector, can be reached before reaching the transition stress τ_t. This stress depends on the relative Schmid factors (f) on each of the partials and R^* which is the ratio of the friction stresses of the two

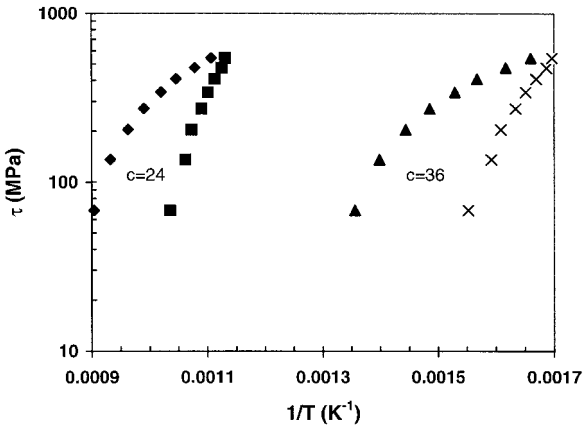

Fig. 11. Logarithm of yield stress as a function of $1/T$ obtained from the relation $\Delta G = ckT$ for 30° glide dislocation (■ and ×) and screw shuffle dislocation (◆ and ▲) for c = 24 and 36. The transition temperature between the two mechanisms is T = 600 °C for c = 24 and T = 315 °C for c = 36

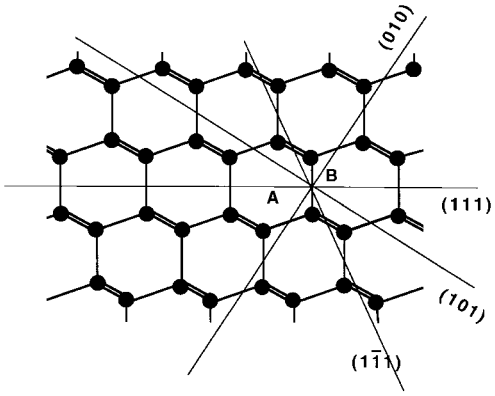

Fig. 12. Location of perfect shuffle dislocations (from Koizumi et al. [21]): A and B. B is the stable one and lies at the intersection of (111) shuffle set and the (1$\bar{1}$1) glide set. The (010) and (101) cross slip planes are also indicated

partials. τ_d is usually lower than τ_t, particularly on the cross slip plane. The minimum value for τ_d is γ/b. In this case the leading partial is the only one submitted to a Peach-Koeler force and its friction force is assumed to be zero ($f = 1$, $R^* = 0$). This minimum value is 0.0022μ far below τ_t, Fig. 10.

– The change from a dissociated glide configuration into a perfect shuffle configuration requires cross slip events. This can be analysed in the light of the atomic calculations of Koizumi et al. [21] who have calculated the stable configurations of shuffle screw dislocations in Si. These calculations show that two types of screw shuffle positions are possible, A and B. B positions are the stable ones (Fig. 12); they are in fact located at the intersection of the (111) plane for a shuffle dislocation and the (1$\bar{1}$1) glide plane for a dissociated glide configuration with the same Burgers vector. They can cross slip on (010) and (101) planes. Then there are two mechanisms that yield to the glide of a perfect shuffle dislocation from a dissociated glide one (Fig. 13). Let us consider a dissociated glide configuration (G), which glides on (111). If there is an obstacle correctly located it can constrict into B_1, a low energy shuffle configuration located on its glide plane. This configuration can then cross slip in its shuffle form on the (1$\bar{1}$1) glide plane provided that this plane possesses a large enough resolved shear stress (larger than τ_t) (G, B_1, A). The second way is a double cross slip mechanism. Indeed, the B_1 constricted shuffle configuration can cross slip on (101) up to a B_2 shuffle config-

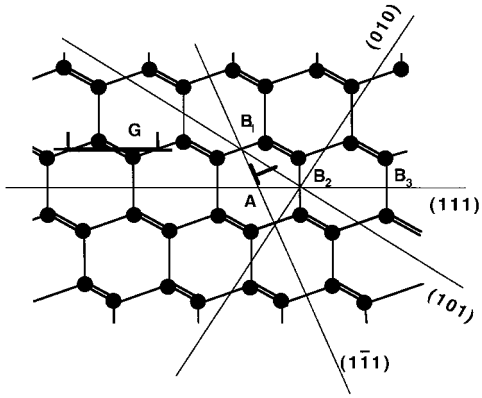

Fig. 13. Paths for a glide-shuffle core transformation of a screw dislocation via cross slip mechanisms. G, B_1, A: cross slip from (111) to (1$\bar{1}$1); G, B_1, B_2, B_3: double cross slip from (111) to (111) via (101)

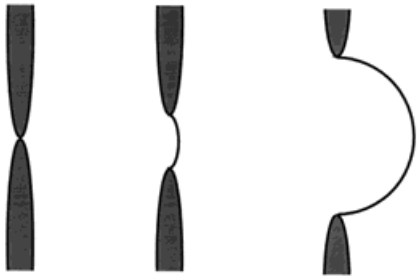

Fig. 14. Cross slip mechanism involved in a glide–shuffle transformation. This mechanism is similar to those proposed for hexagonal metals from basal to prismatic planes [22, 23]

uration located on (111) in which it can cross slip again. Then the shuffle configuration is expected to glide in the plane of maximum resolved shear stress (G, B_1, B_2, B_3).

In these two mechanisms, the elementary step is the cross slip from a dissociated glide configuration into a perfect shuffle dislocation. This is analogous to the cross slip mechanisms proposed by Schoeck and Seeger for fcc metals [22] and by Friedel for hexagonal metals [23] (from basal to prismatic planes, Fig. 14). This type of cross slip requires a large activation energy that has been found unrealistic for fcc metals compared to the Escaig-Friedel mechanism [24]. In the present case a calculation of cross slip events between glide and shuffle configurations should include the Peierls stress in the different planes encountered by the dislocations during their movements. Only atomistic calculations can deal correctly with this problem. It has to be noted that obtaining a critical recombined length of a dissociated glide dislocation, required in the cross slip mechanism, is likely to be very difficult even when the applied stress favours a narrowing of the splitting width. Indeed, by stressing the two partials in order to narrow the stacking fault, Grosbras et al. [25] failed to evidence any recombination, the smaller dissociation width being 6 nm. From these different points it can be deduced that a high activation energy is likely to be required for such a cross slip process and that, at a given temperature, the stress necessary for this mechanism to occur could exceed the transition stress τ_t of the glide–shuffle transition. Furthermore, since for stresses larger than τ_t, glide configurations have a larger activation energy to move than shuffle ones, cross slip of such a glide loop into another glide configuration (which is an easier process than cross slip from glide to shuffle) can lead to glide of dislocations on slip planes with a resolved shear stress lower than τ_t favouring the slip of the glide configuration. In these conditions, dissociated glide dislocations can still control the plastic deformation at resolved shear stresses larger than τ_t.

Comparing with CSC, besides the fact that CSC can be deformed without pre-deformation at low temperatures, constriction of the screw segments which are necessary for the formation of a shuffle dislocation from a glide one are likely to be less difficult on screw segments of CSC compared to those of Si. Particularly in CSC the β/α screw segments are liable to form constrictions more easily, owing to the lower mobility of the leading partial [11]. This has to be taken into account in the glide–shuffle transition.

4. Conclusion

Although yield stresses of the order of magnitude of the calculated critical stress to get a transition between glide and shuffle dislocation cores have already been reached using deformation under a confining pressure, the observed deformation microstructure

has been found to consist of dissociated or widely dissociated dislocations. This bears witness to dislocation movements in the glide set. Such a transition could occur at higher stresses than that extrapolated from calculations [1]. However, obtaining higher yield stresses under reasonable confining pressures (up to 1.5 GPa) requires pre-deformation at higher temperatures which favours the multiplication of glide dislocations. Experiments are in progress to induce plasticity at high stresses without any pre-deformation by using high confining pressures [26].

References

[1] M. S. DUESBERY and B. JOOS, Phil. Mag. Lett. **74**, 253 (1996).
[2] J. CASTAING, P. VEYSSIERE, L. P. KUBIN, and J. RABIER, Phil. Mag. A **44**, 1407 (1981).
[3] J. RABIER, P. VEYSSIERE, and J. L. DEMENET, J. Physique **44**, C4–243 (1983).
[4] J. RABIER, H. GAREM, J. L. DEMENET, and P. VEYSSIERE, Phil. Mag. A **51**, L67 (1985).
[5] P. BOIVIN, J. RABIER, and H. GAREM, Phil. Mag. A **61**, 647 (1990).
[6] Q. REN, B. JOOS, and M. S. DUESBERY, Phys. Rev. B **52**, 13223 (1995).
[7] E. KAXIRAS and M. S. DUESBERY, Phys. Rev. Lett. **70**, 3752 (1993).
[8] A. GEORGE and J. RABIER, Rev. Phys. Appl. **22**, 941 (1987).
[9] T. SUZUKI, T. YASUTOMI, T. TOKUOKA, and I. YONENAGA, Phil. Mag. A **79**, 2637 (1999); phys. stat. sol. (a) **171**, 47 (1999).
[10] P. VEYSSIERE, J. RABIER, M. JAULIN, J. L. DEMENET, and J. CASTAING, Rev. Phys. Appl. **20**, 805 (1985).
[11] J. RABIER and P. BOIVIN, Phil. Mag. A **61**, 673 (1990).
[12] M. CAGNON in: Dislocations et déformation plastique, Les Editions de Physique, Orsay 1980 (p. 55).
[13] H. ALEXANDER, in: Dislocations in Solids, Vol. 7, Ed. F.R.N. NABARRO, North-Holland Publ. Co., Amsterdam 1986 (p. 112).
[14] J. L. DEMENET, Thèse d'Etat, Université de Poitiers (France), 1987.
[15] T. SUZUKI and T. OHMURA, Phil. Mag. A **74**, 1073 (1996).
[16] I. V. GRIDNEVA, YU. V. MILMAN, and V. I. TREFILOV, phys. stat. sol. (a) **14**, 177 (1972).
[17] V. G. EREMENKO and V.I. NIKITENKO, phys. stat. sol. (a) **14**, 317 (1972).
[18] A.V. SAMANT, Ph. D. Thesis, Case Western Reserve University, Cleveland (OH) 1999.
[19] P. PIROUZ, A. V. SAMANT, M. H. HONG, A. MOULIN, and L. P. KUBIN, J. Mater. Res. **14**, 2783 (1999).
[20] K. WESSEL and H. ALEXANDER, Phil. Mag. **35**, 1523 (1977).
[21] H. KOIZUMI, Y. KAMIMURA, and T. SUZUKI, Phil. Mag. A **80**, 609 (2000).
[22] G. SCHOECK and A. SEEGER, Conf. Defects in Solids, Phil. Soc. London 340 (1955).
[23] J. FRIEDEL, Dislocations, Pergamon Press, London 1964 (p. 163).
[24] B. ESCAIG, J. Phys. **29**, 225 (1968).
[25] P. GROSBRAS, J. L. DEMENET, H. GAREM, and J. C. DESOYER, phys. stat sol. (a) **84**, 481 (1984).
[26] J. RABIER, P. CORDIER, J. L. DEMENET, and H. GAREM, to appear in Mater. Sci. Engng. A.